

试验研究

铜基银镀层的导电性及摩擦磨损性能

陈俊寰, 夏延秋, 曹正锋

(华北电力大学能源动力与机械工程学院, 北京 102206)

[摘要] 为了提高电接触材料的导电性能和摩擦学性能,通过电镀方法在铜基体上制备纯银镀层,用回路电阻测定仪测定材料的导电性,采用 MFT-R4000 高速往复摩擦磨损试验机对比铜基体和银镀层在不同润滑条件下的摩擦磨损性能。通过扫描电镜(SEM)观察磨斑表面形貌,采用 X 射线能谱分析仪(EDS)分析磨斑表面的元素组成。结果表明:铜基体上镀银能够提高材料的导电性,其接触电阻最小;脂润滑能够提高铜基体和银镀层的减摩抗磨性能,且银镀层在脂润滑条件下具有优异的摩擦学性能,这归因于银镀层与润滑脂形成的固体-脂复合润滑的减摩和抗磨作用。

[关键词] 银镀层;铜基体;减摩抗磨性;接触电阻;固体-脂复合润滑

[中图分类号] TH117.1 [文献标识码] A [文章编号] 1001-1560(2016)10-0001-04

DOI:10.16577/j.cnki.42-1215/tb.2016.10.001

0 前言

银及银基薄膜在低温、真空环境中具有良好的润滑性能,精密运动部件表面沉积一层较软的银或银基薄膜可以起到有效的减摩抗磨作用^[1,2]。银镀层具有优良的导电性、导热性和可焊性^[3,4]。目前,已研究的低压电器用银基电触头材料有数百种^[5,6]。这些采用电镀银层的电接触部位可以有效降低接触电阻,减少摩擦和提高电接触部位的耐磨性能。但随着科技的发展,对电接触材料的耐磨性提出了更高的要求,单一的银膜润滑很难满足需求。为此,国内外学者做了大量的关于银合金镀层、复合镀层和银基复合材料的研究^[7]。碳纳米管、石墨、二硫化钼、第二相金属等自润滑材料能够显著提高银基复合材料的摩擦学性能,起到良好的减摩抗磨作用^[8~12];但复合镀层工艺相对复杂,导电性能往往低于银基材料^[13,14],并且非金属的加入使镀层表面不够致密,膜基结合强度较差^[15]。第二相的加入可使镀层硬度提高,起到良好的抗磨作用,但在高载荷下,硬度较高的镀层较易发生脆性断裂。类金刚石薄膜和二硫化钼膜都可以与油脂形成固体-油脂复合润滑体系,这种体系具有良好的减摩抗磨作

用^[16,17]。基于银基复合材料的以上缺点和固体-油脂复合润滑的优点,本工作采用电镀的方法制备了铜基银镀层材料,首次研究银镀层-润滑脂复合体系的摩擦磨损和导电性能,以期降低电接触材料接触电阻、提高其耐磨性能提供新思路。

1 试验

1.1 银镀层的制备

选用尺寸 100 mm×50 mm×1 mm 的纯铜作为基体,先用砂纸打磨去除污垢氧化皮,再预镀银使基体表面镀上一层薄银膜: Ag^+ 0.5~1.5 g/L, KCN 30~70 g/L, $\text{K}_2\text{CO}_3 \leq 30$ g/L, 温度 23~28 °C, 电流密度 0.1~0.5 A/dm², 10~30 s。预镀后直接将试片放入镀液中电镀银: Ag^+ 10~60 g/L, KCN 30~80 g/L, K_2CO_3 18~50 g/L, 15~35 °C, 电流密度为 0.1~0.5 A/dm², 搅拌速度 300~1 200 r/min, 1 h。最后用蒸馏水水洗,吹干,即得到所需的铜基银镀层材料,其中纯银镀层厚度约 20 μm。

1.2 测试分析

1.2.1 接触电阻

采用 HLY-200A 型回路电阻测试仪(铜制母排)测量接触电阻。其中,拧紧力矩为 10 N·m,通电时间为 10 s,通电电流为 100 A。

1.2.2 硬度和结合力

用 HX-1000TM/LCD 显微硬度计测量铜基体和银

[收稿日期] 2016-05-19

[通信作者] 夏延秋(1964-),教授,主要从事摩擦学和材料保护的研究,电话:010-61772251, E-mail: xiayanqiu@yahoo.com

镀层的维氏硬度,载荷为 0.1 N,加载时间为 20 s。

根据 GB/T 5270-200X,用弯曲试验定性检测结合力:在 $\phi 1$ mm(试片尺寸为 50 mm \times 100 mm \times 1 mm)的轴上将铜基银镀层试片弯曲 180°,反复弯曲直至断裂。

1.2.3 摩擦磨损特性

采用 MFT-R4000 型高速往复摩擦磨损试验机进行摩擦学性能评价,摩擦副为球盘点接触(摩擦副上试样钢球固定),属滑动摩擦,载荷 5~20 N,往复速度 $v = s \times f$,其中摩擦振幅 s 为 5 mm, f 为往复频率 2~5 Hz。上试样为 AISI 52100 标准试验钢球(0.150~0.350 Si, 0.950~1.050 C, 0.027 P, 1.300~1.650 Cr, 0.200~0.400 Mn,其余是 Fe),硬度为 705~757 HV,表面粗糙度 $R_a = 0.05 \mu\text{m}$,直径为 5 mm。下试样为铜基体材料和镀银材料,试验前和试验后用蒸馏水和石油醚分别超声清洗 10 min。每次试验前涂抹 0.2 g 润滑脂于摩擦副之间。其中,润滑脂是在实验室条件下以聚 α 烯烃(PAO)为基础油,以有机胺和异氰酸酯反应产物作为稠化剂,选择非硫磷型减摩抗磨添加剂制备的聚脲润滑脂(HD-9A)。同时选用进口润滑脂(NB52)作为对比。表 1 给出了 2 种润滑脂的主要性能参数。

表 1 2 种润滑脂的主要性能参数

润滑脂	1/4 锥入度 (0.1 mm)	t (滴 点)/ $^{\circ}\text{C}$	铜片腐蚀 (T3 铜,100 $^{\circ}\text{C}$,24 h)	ρ (体积)/ ($10^{12} \Omega \cdot \text{cm}$)	R (接触)/ $\mu\Omega$	
					初始	终止
HD-9A	82.6	274	1 a	3.53	39.1	38.9
NB52	64.5	286	1 a	4.51	29.8	29.7

摩擦系数由计算机自动记录,磨斑宽度由 NIKON-LV150N 光学显微镜测得。

采用 ZEISS-EVO-18 型扫描电子显微镜(SEM)对试样磨损表面形貌进行观察,并用能谱仪(EDS)对试样磨损表面的主要元素组成进行分析。

2 结果与讨论

2.1 试件的接触电阻

表 2 为基体和银镀层的接触电阻。由表 2 可以看出:银镀层的初始接触电阻和终止接触电阻均比基体的要小,其稳定系数也较基体更接近于 1,这说明银镀层不仅改善了基体材料的导电性能,而且提高了其电流传输的稳定性。

表 2 2 种材料的接触电阻

材料	R (初始)/ $\mu\Omega$	R (终止)/ $\mu\Omega$	稳定系数
铜基体	24.8	24.7	1.003 6
银镀层	20.3	20.3	1.000 0

2.2 试件的硬度和镀层结合力

基体和镀层材料的硬度分别是 103 HV_{0.1N} 和 105 HV_{0.1N}。

根据 GB/T 5270-200X 测试,试件镀层未起皮脱落。

2.3 试件的摩擦磨损性能

2.3.1 摩擦系数和磨斑宽度

图 1 为载荷 10 N、频率 5 Hz 条件下,铜基体和银镀层分别在干摩擦和 2 种润滑脂润滑条件下的平均摩擦系数和磨斑宽度。从图 1a 可以看出:无论是铜基体还是银镀层,干摩擦条件下的摩擦系数明显高于 2 种脂润滑下的摩擦系数;在 NB52 和 HD-9A 润滑下,银镀层的摩擦系数比铜基体的降低了 33.8% 和 48.1%,HD-9A 润滑下银镀层的摩擦系数最小,可达 0.049。从图 1b 看出,与干摩擦相比,脂润滑下 2 种材料的磨斑宽度均较小。在 NB52 和 HD-9A 润滑下,纯银镀层的磨斑宽度比铜基体的分别降低了 28.0% 和 3.0%,HD-9A 润滑下的银镀层磨斑宽度最小,可达 0.359 mm。不难发现铜基体表面镀银层可以和 HD-9A 润滑脂形成固体-脂复合润滑,这种固体-脂复合润滑具有较好的减摩抗磨性能。

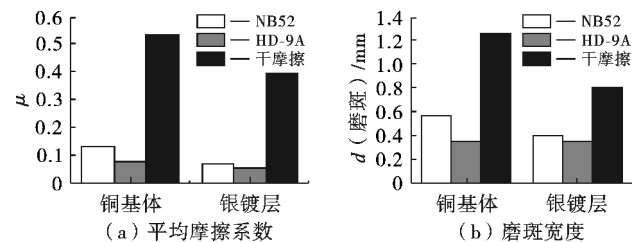


图 1 铜基体和银镀层的平均摩擦系数和磨斑宽度

图 2 为在频率 5 Hz、不同载荷(5, 10, 15, 20 N)条件下,铜基体和纯银镀层分别在 HD-9A 脂润滑和干摩擦条件下的平均摩擦系数和磨斑宽度。从图 2a 可以看出,在所选载荷范围内,纯银镀层在脂润滑(固体-脂复合润滑)下的摩擦系数随着载荷的增大而逐渐增大,在 4 种试验条件下其摩擦系数始终最低,可达 0.037;与铜基体在脂润滑下摩擦情况相比,固体-脂复合润滑下的摩擦系数最高可降低 33.8%;与纯银镀层干摩擦情况相比,最高可降低 87.6%;与铜基体的干摩擦相比,

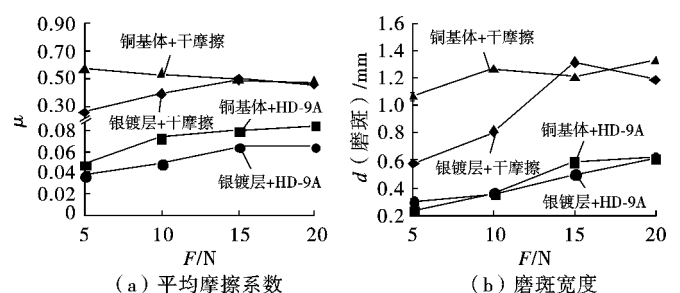


图 2 铜基体和银镀层的平均摩擦系数和磨斑宽度

随载荷变化的曲线

固体-脂复合润滑的摩擦系数最高可降低 93.6% ,固体-脂润滑显示出优异的减摩性能。从图 2b 可以看出,在所选载荷范围内,固体-脂复合润滑下的磨斑宽度随载荷增大而增大;固体-脂复合润滑下的磨斑宽度与脂润滑下的铜基体相差不大,但与干摩擦下的银镀层相比,最高可降低 62.2%;与干摩擦下的铜基体相比,最高可降低 71.8% ,显示出优异的抗磨性能。综上所述,固体-脂复合润滑的减摩抗磨性明显优于单一的脂润滑和固体润滑,更优于干摩擦下的铜基体。

图 3 给出了在载荷为 10 N、不同频率(2,3,4,5 Hz) 试验条件下,铜基体和纯银镀层分别在 HD-9A 脂润滑和干摩擦条件下的平均摩擦系数和磨斑宽度。从图 3a 可以看出,在所选频率范围内,纯银镀层在脂润滑下(固体-脂复合润滑)的摩擦系数先增大后减小,但在 4 种试验条件下其摩擦系数始终最低,可达 0.046;与铜基体在脂润滑下的摩擦情况相比,在固体-脂复合润滑下的摩擦系数最高可降低 40.0%;与纯银镀层干摩擦情况相比,最高可降低 87.6% ,显示出优异的减摩性;与铜基体的干摩擦相比,最高可降低 90.7% ,减摩性能更为优异。从图 3b 可以看出:在所选频率范围内,固体-脂复合润滑的磨斑宽度变化不大,始终保持最低,可达 0.32 mm;与铜基体在脂润滑下相比,固体-脂复合润滑下的磨斑宽度最高可减小 19.3%;与干摩擦下的纯银镀层相比,最高可减小 62.6%;与干摩擦下的铜基材料相比,最高可减小 71.6% 。综上所述,纯银镀层在固体-脂复合润滑下的减摩抗磨性明显优于单一的脂润滑和固体润滑,更优于干摩擦下的铜基体。

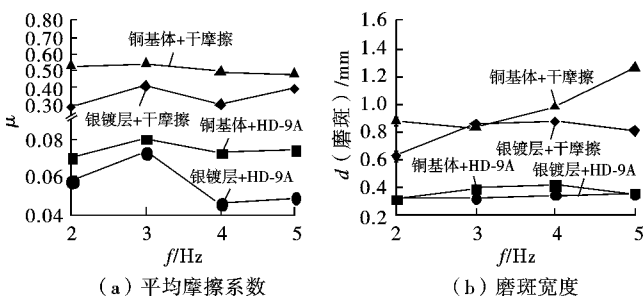


图 3 铜基体和银镀层的平均摩擦系数和磨斑宽度随频率变化的曲线

通过研究载荷和频率对固体-脂复合润滑的减摩性能和抗磨性能的影响,可以发现与单一的银镀层在干摩擦情况下和铜基体在脂润滑下的摩擦情况相比,镀银层和润滑脂可以形成较好的润滑状态,这种固体-脂复合润滑具有优异的减摩性能和抗磨性能。

2.3.2 磨损表面形貌与成分

图 4 为在 HD-9A 润滑脂润滑下(载荷 10 N,频率 5

Hz) 和干摩擦下铜基体和镀银层材料的磨斑表面形貌。干摩擦下铜基体的磨斑宽而深,并且摩擦表面存在大量的金属剥落区域和明显的犁沟(图 4a, 4b)。这主要是由于铜是热的良导体,热容量大,能够把摩擦区域所产生的热量及时地传导带走,保持较高的强度,而钢球试样的热传导能力相对于铜较低,不能及时地将摩擦区域产生的热量带走。因此,造成摩擦表面上聚集较多的热量,导致摩擦表面附近软化,局部区域甚至发生熔化现象,致使接触的峰顶材料发生焊合;此外,在压力作用下摩擦副表面的微凸体压入局部软化的铜块表面,移动时使表面受到严重的塑性变形,压痕两侧材料受到损伤,因而极易从摩擦表面挤出和剥落^[18]。干摩擦下的镀层材料的磨斑较宽,表面有明显的犁沟和剥落区域(图 4c, 4d)。这主要是由于在摩擦开始时,压力作用在较软的银膜上,使银膜相对铜基体滑动,引起摩擦表面的塑性流变,从而改善了摩擦副表面的应力状态,降低了摩擦系数并提高了抗磨性能;随着时间增加,较软的银膜向对偶表面转移,形成转移膜,使摩擦发生在软金属与转移膜之间,从而降低滑动摩擦剪切

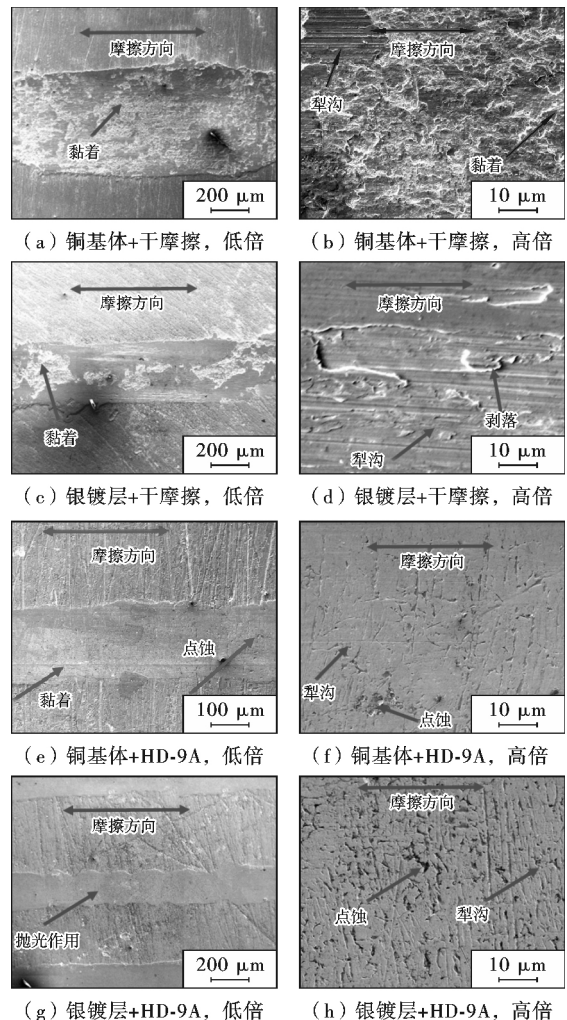


图 4 干摩擦和 HD-9A 条件下两种材料的磨损表面形貌

力,致使摩擦表面黏着磨损程度降低,起到了减摩抗磨作用^[19-20]。脂润滑下铜基体的磨斑窄而浅,表面有轻微刮伤和塑性变形(图4e,4f),这主要是由于在摩擦过程中,由于压力的作用,基础油能够从聚脲润滑脂的纤维结构中析出,起到润滑效果。此外,聚脲分子链上有强极性的脲基基团,其中脲基上的氮原子带有孤对电子,对金属有很强的亲和力,使聚脲润滑脂有序层状结构在金属表面形成的剪切强度远低于金属的吸附膜,防止了摩擦表面直接接触,避免表面发生干摩擦时的黏着磨损^[21-22],但摩擦表面的部分微凸体仍会相互碰撞,产生冲击应力,使微凸体受到重复的冲击和变形,材料受到积累损伤而变弱,最后引起局部材料脱落^[23]。固体-脂复合润滑摩擦表面主要发生轻微塑性变形,磨斑宽度窄且浅,表面光滑(图4g,4h)。这主要是由于固体-脂润滑状态既具有表面镀银层所带来的较好的减摩抗磨特性,也具有脂润滑所起到的减摩抗磨作用,固体-脂复合润滑将这两者较好地结合起来,使镀银层、润滑脂能够在摩擦过程中发挥各自的优势,表现出了协同润滑效应,起到了优异的减摩抗磨作用。

图5为不同条件下磨斑表面的主要元素组成。与干摩擦下铜基体的磨斑表面元素组成相比,HD-9A润滑脂润滑下铜基体的磨斑表面Cu元素含量有所升高,而O元素含量降低。这主要是由于在干摩擦条件下,摩擦行为较为剧烈,在摩擦区域产生大量的热,使铜基体材料被氧化,生成较多的氧化铜;而在聚脲润滑脂润滑下,润滑脂有效地将摩擦副接触表面隔绝起来,并在金属表面形成吸附膜,起到润滑作用,这能有效改善摩擦状况,降低摩擦区域所产生的热量。所以相比于干摩擦,在脂润滑下摩擦表面生成的氧化物较少,因此EDS结果显示O元素含量降低。银镀层在干摩擦条件

下磨斑表面出现Cu元素,主要是由于在干摩擦过程中,摩擦较为剧烈,铜基体表面银镀层被破坏,导致铜基体参与了摩擦过程。相比于银镀层干摩擦,银镀层在聚脲润滑脂润滑下摩擦,其表面仅存在Ag元素和O元素。这主要是由于在摩擦过程中,一方面,镀层表面的银具有自修复作用,能有效参与与摩擦过程中,起到减摩抗磨作用^[24];另一方面,聚脲润滑脂能在表面形成有效润滑保护薄膜,减少摩擦副直接接触,改善摩擦状况。在这二者的共同作用下,降低了摩擦剪切力,有效阻止了镀层的破坏,因此磨斑表面仅出现了Ag元素和O元素。EDS谱分析表明,银镀层-聚脲润滑脂复合润滑有效保护了铜基材料,避免了铜基体参与摩擦过程,改善了摩擦表面的磨损状况,体现了固体-脂复合润滑的协同作用。

3 结论

(1) 银镀层有利于降低铜基体的接触电阻,且能够提高电流传输的稳定性。

(2) 润滑脂能够提高2种材料的减摩抗磨性能,脂润滑下的平均摩擦系数比干摩擦时减小80%左右,磨斑宽度比干摩擦时减小20%左右;固体-脂复合润滑有利于银镀层固体、润滑脂表现出各自的优势,表现出良好的协同润滑效应,具有优异的减摩抗磨性能。复合润滑的摩擦系数比干摩擦下的铜基体减小90%左右,磨斑宽度减小70%左右。固体-脂复合润滑的减摩性能受载荷和频率的共同影响,而其抗磨性能主要受频率的影响。

(3) EDS谱分析表明,固体-脂复合润滑提高了接触副的摩擦学性能,同时提高了摩擦副的抗氧化性能。

[参考文献]

- [1] 高晓明,孙嘉奕,胡明,等. 沉积温度及膜厚对离子镀银膜结构及摩擦学性能的影响[J]. 机械工程材料, 2007(7): 11~14.
- [2] 高晓明,孙嘉奕,胡明,等. 低温沉积Ag-Cu薄膜的耐原子氧和摩擦学性能[J]. 摩擦学学报, 2013(3): 245~252.
- [3] Tyagi R, Dang S X, Li J L, et al. High-temperature friction and wear of Ag/h-BN-containing Ni-based composites against steel[J]. Tribology Letters, 2010, 40(1): 181~186.
- [4] 魏喆良,邵艳群,王欣,等. 铜基材硝酸银溶液浸镀银的沉积过程[J]. 中国有色金属学报, 2008(2): 372~376.
- [5] 马光,孙晓亮. 银基电接触材料改性及制备工艺[J]. 稀有金属快报, 2012, 26(10): 14~19.
- [6] 王松,付作鑫,王塞北,等. 银基电接触材料的研究现状及发展趋势[J]. 贵金属, 2013, 34(1): 79~83.
- [7] Pal H, Sharma V. Thermal conductivity of carbon nanotube-silver composite[J]. Transactions of Nonferrous Metals Society of China, 2015(1): 154~161. (下转第13页)

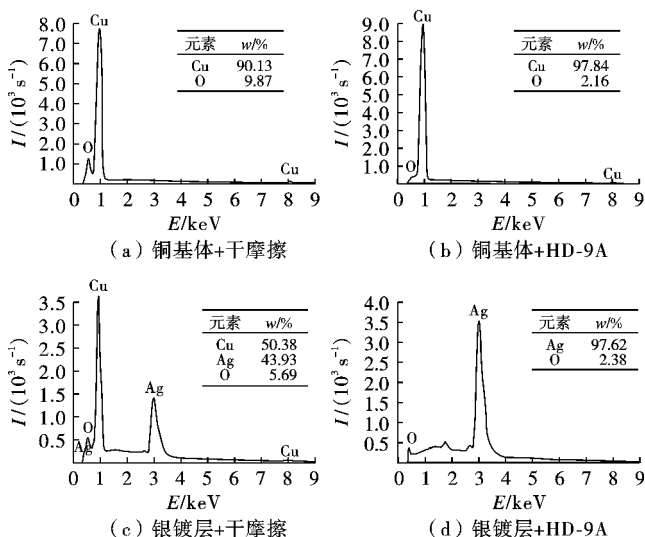


图5 磨斑表面EDS谱

- [10] Stoecker T, Koehler A, Moos R. Why does the electrical conductivity in PEDOT: PSS decrease with PSS content? A study combining thermoelectric measurements with impedance spectroscopy [J]. *Journal of Polymer Science Part B: Polymer Physics*, 2012, 50(14): 976~983.
- [11] Yue R, Xu J. Poly(3,4-ethylenedioxythiophene) as promising organic thermoelectric materials: A mini-review [J]. *Synthetic Metals*, 2012, 162(11/12): 912~917.
- [12] Pournaghi-Azar M H, Habibi B. Electropolymerization of aniline in acid media on the bare and chemically pre-treated aluminum electrodes, a comparative characterization of the polyaniline deposited electrodes [J]. *Electrochimica Acta*, 2007, 52(12): 4222~4230.
- [13] Sazou D, Georgolios C. Formation of conducting polyaniline coatings on iron surfaces by electropolymerization of aniline in aqueous solutions [J]. *Journal of Electroanalytical Chemistry*, 1997, 429(1/2): 81~93.
- [14] Kulkarni M V, Viswanath A K, Marimuthu R, et al. Synthesis and characterization of polyaniline doped with organic acids [J]. *Journal of Polymer Science: Part A: Polymer Chemistry*, 2004, 42(8): 2043~2049.
- [15] Gospodinova N, Mokreva P, Terlemezyan L. Chemical oxidative polymerization of aniline in aqueous medium without added acids [J]. *Polymer*, 1993, 34(11): 2438~2439.
- [16] Lukachova L V, Shkerin E A, Puganova E A, et al. Electro-
- activity of chemically synthesized polyaniline in neutral and alkaline aqueous solutions role of self-doping and external doping [J]. *Journal of Electroanalytical Chemistry*, 2003, 544(13): 59~63.
- [17] Focke W W, Wnek E G, Wei Y. Influence of oxidation state, pH, and counterion on the conductivity of polyaniline [J]. *The Journal of Physical Chemistry*, 1987, 91(22): 5813~5818.
- [18] Tahir Z M, Alcolija E C, Grooms D L. Polyaniline synthesis and its biosensor application [J]. *Biosensors and Bioelectronics*, 2005, 20(8): 1690~1695.
- [19] Reda S M, Al-Ghannam S M. Synthesis and Electrical Properties of Polyaniline Composite with Silver Nanoparticles [J]. *Advances in Materials Physics and Chemistry*, 2012, 2(2): 75~81.
- [20] Liao C, Gu M. Electroless deposition of polyaniline film via autocatalytic polymerization of aniline [J]. *Thin Solid Films*, 2002, 408(1/2): 37~42.
- [21] Marian I, Oniciu L. Characterization of polyaniline by cyclic voltammetry and UV-Vis absorption spectroscopy [J]. *Journal of Materials Science*, 1999, 34(11): 2733~2739.
- [22] Gao H, Jiang T, Han B, et al. Aqueous/ionic liquid interfacial polymerization for preparing polyaniline nanoparticles [J]. *Polymer*, 2004, 45(9): 3017~3019.

[编校: 郑霞]

(上接第4页)

- [8] 凤仪, 张敏, 徐屹. 外加载荷对碳纳米管-银-石墨复合材料电磨损性能的影响 [J]. *中国有色金属学报*, 2005(10): 7~12.
- [9] 张敏, 凤仪. 电流对碳纳米管-银-石墨复合材料摩擦磨损性能的影响 [J]. *摩擦学学报*, 2005(4): 328~332.
- [10] 徐屹, 凤仪, 王松林, 等. 碳纳米管-银-石墨复合材料的电磨损性能 [J]. *机械工程学报*, 2006(12): 206~210.
- [11] 王新平, 肖金坤, 张雷, 等. 银合金粉末粒度对 Ag-MoS₂ 复合材料摩擦磨损性能的影响 [J]. *中国有色金属学报*, 2012(10): 2811~2817.
- [12] 刘道新, 王振亚, 张晓化, 等. Ag/Ni 多层膜对钛合金微动磨损和微动疲劳抗力的影响 [J]. *摩擦学学报*, 2010(5): 498~504.
- [13] 邓书山, 王文芳, 吴玉程, 等. 银基复合材料电刷的导电性能 [J]. *机械工程材料*, 2007(4): 55~57.
- [14] 布朗洛维克, 康奇兹, 米西金. 电接触理论、应用与技术 [M]. 北京: 机械工业出版社, 2010: 78~109.
- [15] 胡明, 张立平, 高晓明, 等. Cr/Ag 纳米多层薄膜膜-基结合强度及摩擦学性能研究 [J]. *摩擦学学报*, 2012(6): 544~549.
- [16] 郝俊英, 翁立军, 孙嘉奕, 等. 固体-油脂复合润滑 I: 二硫化钼膜在干摩擦及空间用油脂润滑下的摩擦学性能 [J]. *摩擦学学报*, 2010, 30(2): 105~110.
- [17] 郝俊英, 王鹏, 刘小强, 等. 固体-油脂复合润滑 II: 类金刚石(DLC)薄膜在几种空间用油脂润滑下的摩擦学性能 [J]. *摩擦学学报*, 2010(3): 217~222.
- [18] 王观民, 张永振, 杜三明, 等. 不同气氛环境中钢/铜摩擦副的高速干滑动摩擦磨损特性研究 [J]. *摩擦学学报*, 2007(4): 346~351.
- [19] Holmberg K, Ronkainen H, Mattews A. Tribology of thin coatings [J]. *Ceramics International*, 2000, 26: 787~795.
- [20] 金杰, 邱维维, 王锦辉, 等. IBAD 和磁控溅射对银膜性能的影响 [J]. *核技术*, 2010(12): 918~922.
- [21] 栗志彬, 董禄虎, 高艳青. 聚脲润滑脂研究现状及发展趋势 [J]. *石油商技*, 2013(5): 18~22.
- [22] 曹珍, 王文, 陶德华, 等. 润滑油添加剂摩擦学性能的试验研究 [J]. *轴承*, 2010(6): 32~34.
- [23] Fan X Q, Xia Y Q, Wang L P, et al. Study of the Conductivity and Tribological Performance of Ionic Liquid and Lithium Greases [J]. *Tribology Letters*, 2014, 53(1): 281~291.
- [24] 杨绿, 周元康, 李屹, 等. 坡缕石/Ag 复合纳米材料添加剂的自修复性能研究 [J]. *材料工程*, 2012(3): 12~16.

[编校: 郑霞]



Contents & Abstracts

Conductivity and Tribological Properties of Electroplated Silver Coating Based on Copper Substrate

CHEN Jun-huan, XIA Yan-qiu, CAO Zheng-feng (School of Energy Power and Mechanical Engineering, North China Electric Power University, Beijing 102206, China). *Cailiao Baohu* 2016, 49(10), 01~04 (Ch). In order to improve the conductivity and tribological properties of electrical contact materials, silver coating was prepared by electroplating on copper substrate. The electrical conductivity of coating was tested by circuit resistance tester, and the tribological property was evaluated by high speed reciprocating friction and wear tester, respectively. In addition, the scanning electron microscopy (SEM) and energy-dispersive X-ray spectroscopy (EDS) were employed to analyze the wear surfaces and typical elements. Results showed that the silver plating could improve the conductivity of the substrate material and obtain the lowest contact resistance. Lubricating greases could improve antifriction and wear resistance property, and the silver coating under lubrication conditions had the best tribological performance, owing to the antifriction and wear influence of solid film/grease composite lubrication.

Key words: electroplated silver coating; copper substrate; antifriction and wear resistance; contact resistance; solid film/grease composite lubrication

Corrosion Behaviours of Thermal Spraying Aluminium Coating for Offshore Engineering

LIU Cun¹, ZHAO Wei-min², CHEN Hong-yu³ (1. Offshore Oil Engineering (Qingdao) Company Ltd., Qingdao 2665200, China; 2. China University of Petroleum, Qingdao 266500, China; 3. Research Center of CNPC Fushun Petrochemical Equipment Inspection and Supervision, Fushun 113000, China). *Cailiao Baohu* 2016, 49(10), 05~08 (Ch). Aluminum coating was deposited on Q235 steel substrate by using thermal spraying, based on the application of thermal spraying aluminum coating (TSA) on the offshore steel structures. Electron probe micro-analysis (EPMA) was used to analyze the element distribution features of Al, O, Cl and Fe of the coating cross-section after immersed in 3.5% NaCl aqueous solution for 30 d. The potentiodynamic polarization curve was used to test and fit the corrosion current density of coating before and after hanging strip corrosion test. Moreover, the coating electrochemical corrosion failure process was studied by electrochemical impedance spectroscopy (EIS). Results showed that corrosion medium could penetrate into the inner coatings along the pores or inclusions, observed by EPMA. The original coating potentiodynamic polarization proved obvious passivation phenomenon of Al coating, which was related to the strong adhesion of corrosion products $Al(OH)_3$ and the existence of Al_2O_3 film. During the test process, the EIS of Al coating presented four stages of pitting initiation, acidified hydrogen in pits, coating becoming sacrificial anode and rapid development of pits cluster, and the equivalent circuit models of impedance corresponding to each stage were fitted by ZsimpWin software.

Key words: thermal spraying aluminum coating; corrosion electrochemistry; offshore engineering; steel structures; electrochemical impedance spectroscopy

Effects of Different Anions on Aniline Electropolymerization

LIU Xiao-qing, WANG Wei (School of Chemical Engineering and Technology, Tianjin University, Tianjin 300072, China). *Cailiao Baohu* 2016, 49(10), 09~13 (Ch). It is reported that the struc-

tures and properties of polyaniline materials have close connection with polymerization conditions. During the process of aniline electropolymerization, different anions have varying degree of influences on the nucleation and the formation rate of polyaniline films. The aniline electropolymerization process was studied by cyclic voltammograms (CV) and electrochemical impedance spectrometry (EIS) on the Au electrode in different acid solutions doped with anions such as NO_3^- , SO_4^{2-} , Cl^- , ClO_4^- and PO_4^{3-} . Subsequently, the principles of polymerization were further analyzed by using the proposed electrical equivalent circuits. Results showed that the key step for aniline electrodeposition was the oxidation of monomer aniline to its cation radicals, and the order from difficulty to easiness of the anions dissolved in different electrolytes for aniline oxidation to cation radical was $NO_3^- > SO_4^{2-} > ClO_4^- > Cl^- > PO_4^{3-}$. Particularly, the reaction had the lowest resistance in the solution contained PO_4^{3-} , due to the notable catalytic effect of PO_4^{3-} .

Key words: electropolymerization; polyaniline; anions; electrochemistry

Inhibition Effect of N-(2-Hydroxypropyl) Chitosan Doped Polyaniline on Carbon Steel in 0.5 mol/L HCl

GUO Ying, LIU Bo (College of Science, Civil Aviation University of China, Tianjin 300300, China). *Cailiao Baohu* 2016, 49(10), 14~17 (Ch). N-(2-hydroxypropyl) chitosan doped polyanilines (HPCS-PANI) were synthesized by chemical oxidation method with using N-(2-hydroxypropyl) chitosan (HPCS) and aniline (An). Subsequently, the products were characterized by Fourier transform infrared spectroscopy (FTIR), which proved that the products were HPCS-PANI. Then weight-loss method and electrochemical method were applied to study the corrosion inhibition of HPCS upon Q235 mild steel in 0.5 mol/L HCl. Results showed that HPCS-PANI could be used as an absorptive inhibitor which complied with Langmuir adsorption isotherm upon carbon steel surface. When the concentration was 50 mg/L, the inhibitor efficiency of HPCS-PANI on Q235 carbon steel could reach the maximum 88.94% in 50 mg/L.

Key words: inhibitor; N-(2-hydroxypropyl) chitosan; polyaniline; weight-loss method; electrochemistry; Q235 carbon steel

Effects of Direct Stray Current on Surface Morphology and Electrochemical Behavior of X65 Steel

YANG Chao, CUI Gan, LI Zi-li, ZHANG Cheng-bin, ZHAO Ya-lei (Provincial Key Laboratory of Oil and Gas Storage and Transportation Security, College of Pipeline and Civil Engineering, China University of Petroleum, Qingdao 266580, China). *Cailiao Baohu* 2016, 49(10), 18~22 (Ch). In order to explore the interference effect of direct stray current on the corrosion of pipeline, three electrodes system was built to test polarization curves and electrochemical AC impedance spectra (EIS) of working electrode under various DC conditions, and the morphology of corrosion surface was observed by confocal microscope and stereoscopic microscopes. Results showed that with direct stray current density increasing, the corrosion potential and corrosion current density increased. However, when the DC density reached to $100 A/m^2$, working electrode was passivated, and the corrosion potential and corrosion rate declined. With applied current density increasing, the inductance loop disappeared gradually and turned into Warburg impedance. When DC current density reached to